Proc Indian Natn Sci Acad **79** No. 4 December 2013 Spl. Issue, Part A, pp. 687-694

DOI: 10.16943/ptinsa/2013/v79i4/48000

Research Paper

Response of Containment Subjected to Missile Penetration

B S SHARMA[1*], M A IQBAL[2], P BHARGAVA[2] and P GUNDLAPLLI[1]
[1]*Nuclear Power Corporation of India Limited, Anushakti Nagar, Mumbai 400 094, India*
[2]*Department of Civil Engineering, Indian Institute of Technology, Roorkee 247 667, Uttarakhand, India*

(Received 31 January 2013; Accepted 26 March 2013)

Finite element analysis has been carried out to study the response of reinforced concrete containment subjected to direct impact of a missile. The effect of penetration of the missile on containment is evaluated. The missile impact is considered to occur at two different locations i.e., (a) junction of dome and cylinder, and, (b) mid-height of the cylindrical portion. The damaged plasticity model is used to incorporate material behaviour of concrete, and Johnson-Cook elasto-viscoplastic material model is used to incorporate material behaviour of steel reinforcement. The missile velocity is considered in the range of 100 m/s and 200 m/s. To obtain the strain rate dependency of simulation results, strain rate dependent and strain rate independent material models are used for the same geometric model. 40% decrement in the penetration value, due to incorporation of strain rate effect is observed. For a given impact velocity, the penetration depth and damage intensity are found to be higher at the junction of dome and cylinder as compare to that of mid-height of cylindrical portion. This study indicated that the containment is capable to resist the impact of the missile under consideration.

Key Words: Concrete Containment; Missile; Strain Rate; Concrete-Damage Plasticity; Blast Loading; Elasto-Visco Plastic Model

1. Introduction

Abbas *et al.* [2] studied the response of outer containment for different aircraft impacts at different locations of containment. Strain rate dependent elasto-viscoplastic model was used in the analysis, and considering the target as rigid in the analysis this assumption was found as non-conservative and unrealistic. Kukreja [7] found the response of double containment structure for aircraft impact. Nonlinear material model for materials were used. The loading time history for aircraft was applied on the structure to find the response. Local cracking of concrete was found in inner containment, perforation of outer containment was observed in the analysis results. Li *et al.* [8] studied the local impact effects of hard missile penetrating on concrete targets. Empirical, analytical and numerical studies were conducted. Strain rate effect has been incorporated in the material model of concrete in order to perform numerical simulation. The results obtained from empirical, analytical and numerical studies were compared with the results obtained from SHPB (Split Hopkinson Pressure Bar) test. Very few studies are available in which the response of RC structure subjected to missile impact has been studied. The present study is an attempt to find the response of containment for missile penetration.

The study involved geometric modelling of the missile and target, modelling of non-linear behaviour of materials and estimation of blast load. A 3D finite element model of a typical concrete containment is made. The analysis is carried out using ABAQUS/ Explicit [1] finite element code. The material behaviour of concrete is incorporated using damage plasticity model, which is based on the concept of isotropic damaged elasticity in conjunction with

**Author for Correspondence: E-mail: bhavanishanker.iitr@gmail.com*

isotropic tensile and compressive plasticity. The material behaviour of steel is incorporated using Johnson-Cook Elasto-viscoplastic Material Model. Two different locations for impact are considered, viz., (a) midpoint of the cylindrical portion, and, (b) springing point (junction of dome and cylinder). The incidence angle of impact has been considered normal to the containment surface. Penetration study is conducted for two critical locations.

2. Finite Element Modelling

The numerical simulation of concrete containment subjected to missile penetration is carried out using ABAQUS/Explicit-6.9.3 [1] finite element code. A three-dimensional model of the containment is made using preprocessing module of the code. The base of the containment is assumed as fixed. Typical geometry and reinforcement detailing (as per Table 1) of containment has been considered. The typical missile geometry of CRH value 2.176 and a weight of 462 kg are considered (based on the preliminary studies carried out), are shown in Fig. 1. The containment structure had a cylindrical wall with 0.6 m thickness and a spherical dome with 0.25 m thickness, other details are as shown in Fig. 2. The missile impact is considered to occur at two different locations i.e., the junction of dome and cylinder and the centre of the cylindrical portion, Fig. 2. The structure is reinforced in orthogonal directions, at the inner and outer faces of the cylindrical wall and dome; details of reinforcement are presented in Table 1. The effective cover to the concrete is assumed as 70mm. Perfect bond between reinforcing steel and concrete is assigned in the model.

The containment structure is divided into four regions to enable appropriate meshing, i.e., core impact region, region near to core region, dome portion and cylindrical portion, as shown in Fig. 3(a). The containment structure is meshed with Continuum three dimensional reduced integration eight node elements (C3D8R of ABAQUS) in region 1, 3 and 4. The portion between the core and outer region i.e., region 2, identified as transition region, is meshed with tetrahedral elements (C3D4 of ABAQUS). A mesh convergence study is carried out to obtain accurate results within the optimum computational time. The penetration analysis is carried out on the containment with three types of meshes, the details of the element sizes at different regions are shown in Table 2. It is

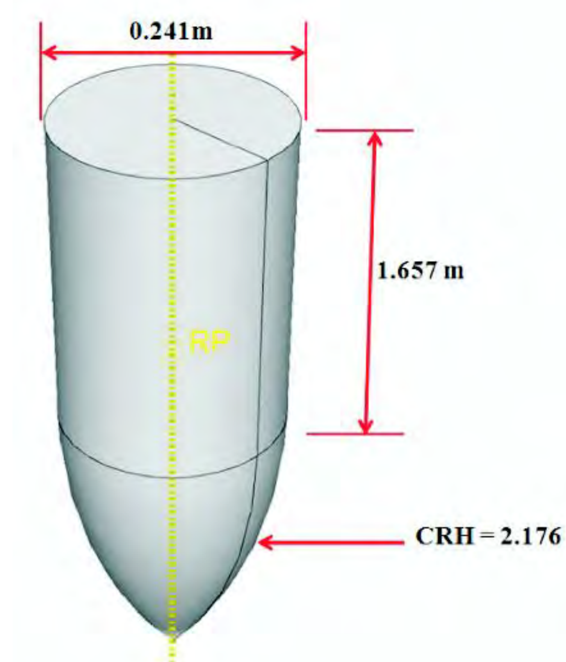

Fig. 1: Missile geometry

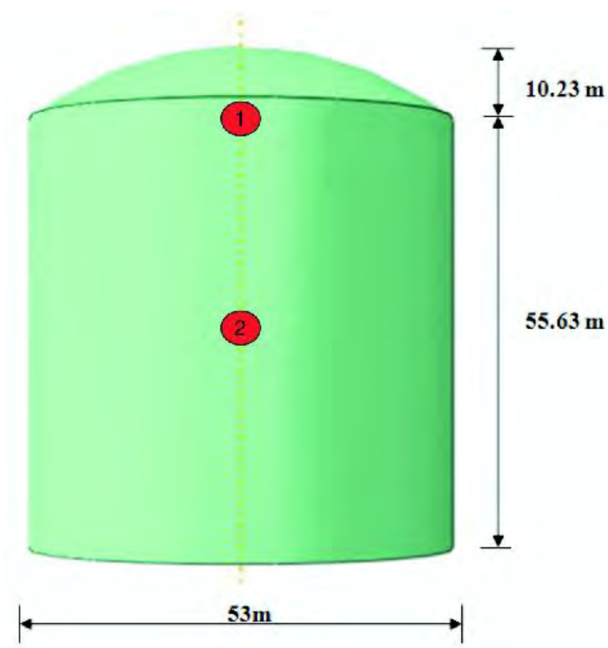

Fig 2: Dimensions of RC Containment and impact locations 1 and 2

Table 1: Reinforcement details of containment

Region	Direction	Inner face	Outer face
Cylindrical	Longitudinal	2×28 mm dia @200 mm c/c	32 mm dia @200 mm c/c
	Hoop	28 mm dia @200 mm c/c	28 mm dia @200 mm c/c
Dome	Direction 1	16 mm dia @200 mm c/c	16 mm dia @200 mm c/c
	Direction 2	16 mm dia @200 mm c/c	16 mm dis @200 mm c/c

Table 2:. Element sizes for Type 1, Type 2 and Type 3 meshing

Region	Element type	Size of element (m)		
		Type-1	Type-2	Type-3
1	C3D8R	0.05	0.1	0.2
2	C3D4	0.05	0.1	0.2
3	C3D8R	0.3	0.6	0.6
4	C3D8R	0.25	0.25	0.25

observed that, there is 2% variation in the displacement value of the missile for Type 2 mesh as compared to that observed for Type 1 Thus the optimum coarser mesh, i.e., Type 2 mesh is adopted for the penetration analysis (as shown in Fig. 3(b)).

3. Constitutive Modelling

(a) Constitutive Model for Steel

The material behaviour of the steel reinforcement is incorporated using Johnson-Cook elasto-viscoplastic material model [6]. This model can incorporate the fracture behaviour of the ductile materials under dynamic loading conditions. This model considers the dependency of von-mises stress $\bar{\sigma}$ on different parameters like strain rate, temperature, stress tri-axiality and plastic flow. The equivalent von-mises stress $\bar{\sigma}$ of the Johnson-Cook model is expressed as:

$$\bar{\sigma}(\bar{\varepsilon}^{pl}, \dot{\bar{\varepsilon}}^{pl}, \hat{T}) = [A + B(\bar{\varepsilon}^{pl})^n]\left[1 + C\ln\left(\frac{\dot{\bar{\varepsilon}}^{pl}}{\varepsilon_0}\right)\right][1 - \hat{T}^m] \tag{1}$$

where, 'A' is quasi-static yield stress, 'B' is a hardening constant, 'n' is the hardening exponent, 'C' is the strain-rate sensitivity parameter and m is the temperature sensitivity parameter. $\bar{\varepsilon}^{pl}$ is the equivalent plastic strain, $\dot{\bar{\varepsilon}}^{pl}$ is equivalent plastic strain rate, is a reference strain rate and $\hat{T}$ is non dimensional temperature defined as:

$$\hat{T} = (T - T_0)/T_{\text{melt}} - T_0) \quad T_0 \le T \le T_{\text{melt}} \tag{2}$$

where, T is the current temperature, T_{melt} is the melting temperature and T_0 is the room temperature. The equivalent fracture strain $\bar{\varepsilon}_f^{pl}$ is expressed in the following form:

$$\bar{\varepsilon}_f^{pl}\left(\frac{\sigma_m}{\bar{\sigma}}, \dot{\bar{\varepsilon}}^{pl}, \hat{T}\right) = \left[D_1 + D_2\exp\left(D_3\frac{\sigma_m}{\sigma}\right)\right] \times\left[1 + D_4\ln\left(\frac{\dot{\bar{\varepsilon}}^{pl}}{\varepsilon_0}\right)\right][1 + D_5\hat{T}] \tag{3}$$

where, D_1-D_5 are material parameters, $\frac{\sigma_m}{\bar{\sigma}}$ is the stress tri-axiality ratio and σ_m is the mean stress. The material parameters of reinforcing steel (as given in Table 3) are considered identical to those of the Weldox 460 E steel obtained by Borvik *et al.* [3].

(b) Constitutive Model for Concrete

Damage plasticity model is used to incorporate the behaviour of concrete in the simulation. This model is suitable for dynamic loading conditions of material, as it can incorporate the strain rate dependent behaviour of concrete. Inelastic behaviour of concrete is represented by using isotropic damaged elasticity in conjunction with isotropic tension and compression plasticity. Tensile cracking and compression crushing

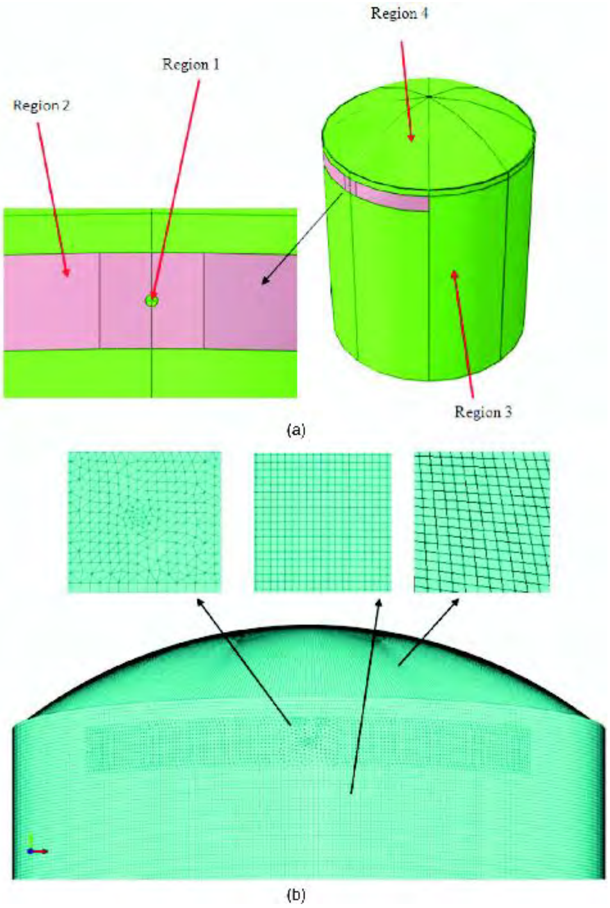

Fig. 3: (a): Four regions of meshing for position 1, (b): Type 2 mesh

are assumed as the main failure mechanisms of concrete. Under uniaxial Tension, tensile cracking beyond the failure stress (σ_{t0}) is defined by representing the micro-cracks macroscopically with a softening stress-strain response, as shown in Fig. 4(a). Under uniaxial compression, beyond first yield point (σ_{c0}), stress hardening is defined until ultimate stress point (σ_{cu}), followed by the strain softening, as indicated in Fig. 4(b). When the concrete is subjected to cyclic loading, its' elastic stiffness decreases in the strain softening region. This degradation of stiffness is observed in compression and tension behaviour of concrete, which is considered as the damage in the material in this model.

The stress-strain relations under uniaxial tension and compression loading with damage parameters d_t and d_c are as follows

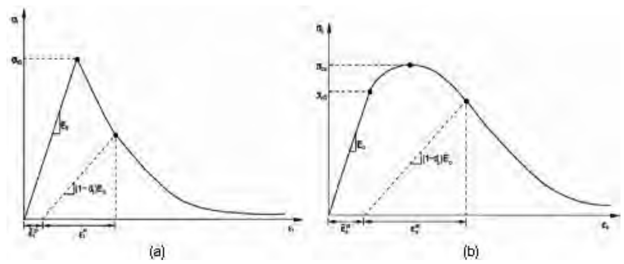

Fig. 4: Response of concrete to uniaxial loading (a): in compression, (b): in tension

$$\sigma_t = (1-d_t)E_0(\varepsilon_t - \tilde{\varepsilon}_t^{pl}) \quad (4)$$

$$\sigma_c = (1-d_c)E_0(\varepsilon_c - \tilde{\varepsilon}_c^{pl}) \quad (5)$$

where, the subscripts 't' and 'c' refer to tension and compression respectively, $\tilde{\varepsilon}_t^{pl}$ and $\tilde{\varepsilon}_c^{pl}$ are the equivalent plastic strains, and is the initial elastic modulus of concrete.

Table 3: Johnson-Cook hardening and dynamic failure parameters, Borvik *et al.* [3]

Young's modulus; E (N/ mm^2)	2 x 10^5
Poisson ratio, ∂	0.33
Density, P (Kg/m^3)	7850
Yield stress, A (N/mm^2)	490
B (N/ mm^2)	383
N	0.45
Reference strain rate (s^{-1})	5x10^{-4}
C	0.0114
M	0.94
T_{melt} (K)	1800
T_0 (K)	293
Specific heat Cp (J/ Kg K)	452
Inelastic heat fraction, α	0.9
D1	0.0705
D2	1.732
D3	–0.54
D4	–0.01
D5	0.0

The reinforcing steel interrupts the tension cracking of the concrete; this effect is incorporated as tension stiffening in the model. The tension stiffening data can be given in two ways; (a) either directly giving the stress-strain curve after failure point (σ_{t0}) or, (b) by giving fracture energy (G_f) vs displacement curve using Hillerborg's fracture energy criterion [5]. In the present study, fracture energy criterion is used, vide Fig. 5.

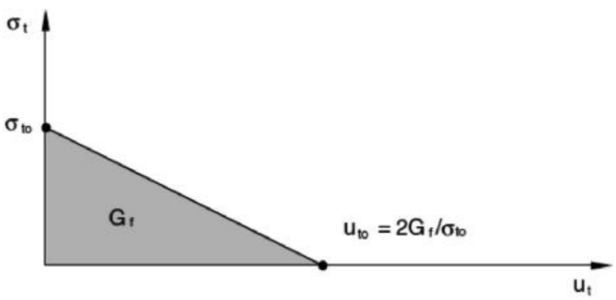

Fig. 5: Post-failure Stress-Fracture Energy Curve

To obtain the strain rate dependency of simulation results, strain rate dependent and strain rate independent material models are used for the same geometric model. Firstly, strain rate independent material model is used; at a later stage of analysis, the model is revised to incorporate strain rate effect. For strain rate independent concrete model, compression behaviour is defined by employing the cyclic stress-strain curve presented by Sinha *et al.* [10], vide Fig. 6. Tension behaviour is defined using the results of experiment conducted by Wolinski *et al.* [11]. Sinha *et al.* [10] conducted experiments on concrete specimens (compressive strength 25.8 MPa) under low strain rate cyclic loading, to obtain the stress-strain response in the plastic zone. Plastic strain is obtained for representative points on the strain softening branch. The Stiffness degradation of each point on the strain softening branch is calculated using the plastic strain value. Wolinski *et al.* [11] conducted experiments on prismatic concrete specimens of size 150 mm by 60 mm by 50 mm, to find the influence of aggregate size on fracture energy of concrete. The fracture energy value for 16 mm aggregate size of 30 MPa concrete is considered in the analysis.

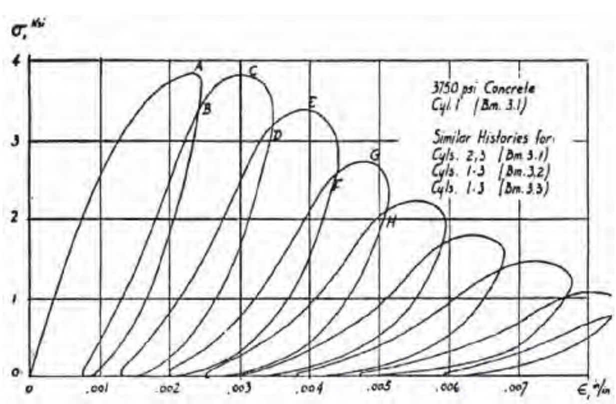

Fig. 6: Compressive stress strain curves for cyclic loading. Sinha *et al.* [10]

For strain rate dependent analysis, the stress-strain relations of concrete was obtained from experiment results of Groute *et al.* [4] based on quasi-static tests on cylindrical specimens (of diameter 3 in. and length of 6 in.), as shown in Fig. 7. In the present study, the strain rate of the elements near to the impact portion is observed as 625 sec^{-1}, hence, the stress-strain curve corresponding to a strain rate of 625 sec^{-1} is employed.

Lu and Xu [9] performed analytical study on uniaxial tension behaviour of concrete at high strain rate. The ratio of dynamic strength to static strength of concrete under different strain rates obtained by Lu and Xu [9] is used to incorporate the tension stiffening in the model, Fig. 8. At 600 sec^{-1} strain rate, the dynamic strength of concrete has increased by 8 times to that of its static strength. Therefore, the

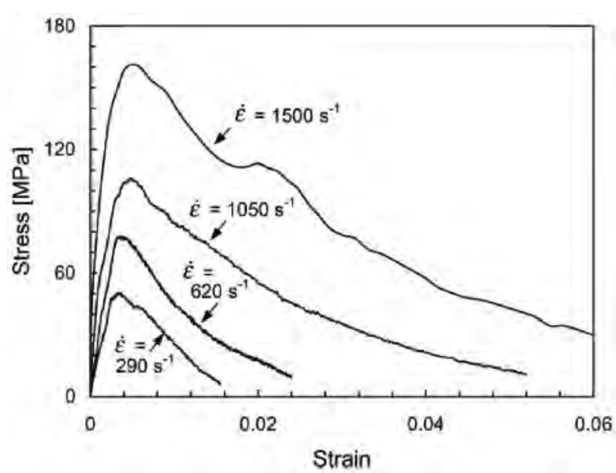

Fig. 7: Compressive stress-strain curves for different values of strain rate, Groute *et al.* [4]

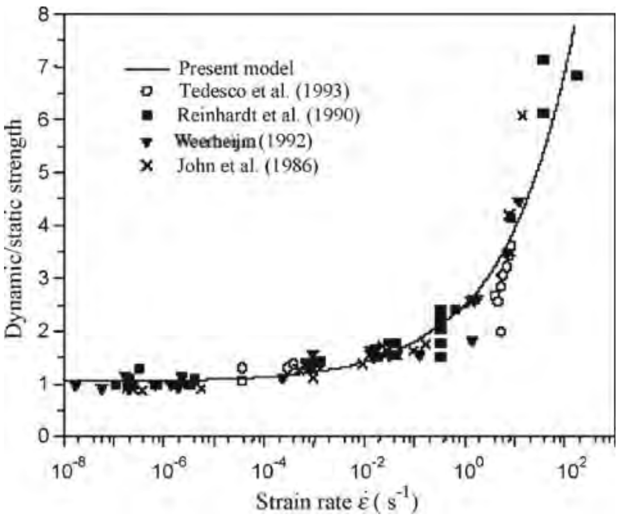

Fig. 8: Graph between dynamic strength ratio and strain rate for concrete under uniaxial tension, Lu and Xu [9]

fracture energy of concrete has been increased by eight times in the strain rate dependent data. The material parameters of the concrete damaged plasticity model are summarized in Table 4.

Table 4: Concrete damaged plasticity parameters

Density, ρ (kg/m^3)	2400
Modulus of elasticity, E (N/m^2)	2.7386E+10
Poisson's ratio, ∂	0.17
Dilation angle, ψ	29^0
Eccentricity (m)	1.0
Initial equi-biaxial compressive yield stress to initial uniaxial compressive yield stress, f_{b0}/f_{c0}	1.16
Bulk modulus, K	0.666
Viscosity parameter	0
Fracture energy, G_f (N/m)	720
Uniaxial failure stress, σ_{t0} (MPa)	10.8
Cracking displacement, U_{t0} (m)	0.0001332
Tensile strength, σ_{st} (MPa)	3.86
Compressive strength (MPa)	25

4. Results and Discussion

a) Strain Rate Effect

The numerical analysis is performed to find the penetration of missile on the containment with strain rate independent and strain rate dependent concrete model. Difference in response of structure is studied in detail. The Impact location at the centre of cylindrical portion of the containment is considered for this purpose. The initial velocity of missile is taken as 200 m/s. The effect of strain rate on the results is presented in terms of penetration depth. Fig. 9 shows displacement history of missile for the strain rate dependent model and strain rate independent model. The displacement of missile is found to be 0.85m in case of strain rate independent model, whereas, the displacement of 0.5m is observed in case of strain rate dependent model. This implies that, there is 40% decrement in the displacement value, due to incorporation of strain rate effect. The missile reached its maximum displacement at 0.04 sec in case of strain rate independent model; however, in case of strain rate dependent model this time is found to be 0.01sec.

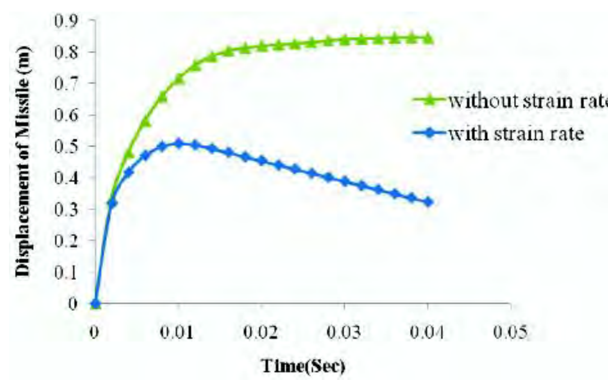

Fig. 9: Strain rate effect on the displacement history of missile

b) Penetration of Containment

The finite element model of containment with the strain rate dependent concrete model is analyzed for the penetration of missile at two different locations, i.e., (a) junction of cylinder and dome, and, (b) centre of cylinder with the two different velocities i.e 100 m/s and 200 m/s. Fig. 10 shows displacement history of missile at two different locations for two different

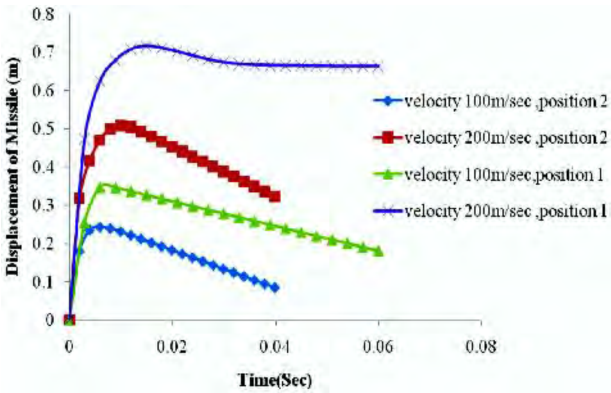

Fig. 10: Displacement history of missile for different positions and velocities

velocities. It is observed that, for the same missile velocity, missile penetrated to a higher depth in impact location (1) than that for location (2).

The distribution of the initial kinetic energy of the missile to different forms of energies in the impact process is shown in Table 5, for different locations of impact for 200 m/s missile velocity. From Table 5, it can be deduced that damage dissipation energy is more in impact location 1, which indicates an intensive damage at that location, plastic dissipation energy is found to be more in location 2, which indicates distribution of damage to a larger area. Fig. 11 shows the penetration of missile into containment wall at two locations with 200 m/s velocity. Missile came to rest in both of these cases. Hence, it can be concluded that the containment is safe against the missile impact considered in this study.

Table 5: Energy distribution in impact process

Energy type	Percentage of initial kinetic energy	
	Location 1, 200 m/s	Location 2, 200 m/s
Artificial energy	18	2.9
Damage dissipation energy	1.6	4.17
Frictional dissipation energy	21	19
Plastic dissipation energy	54	71
Strain energy	0.3	0.98
Viscous dissipation energy	3.5	2.73

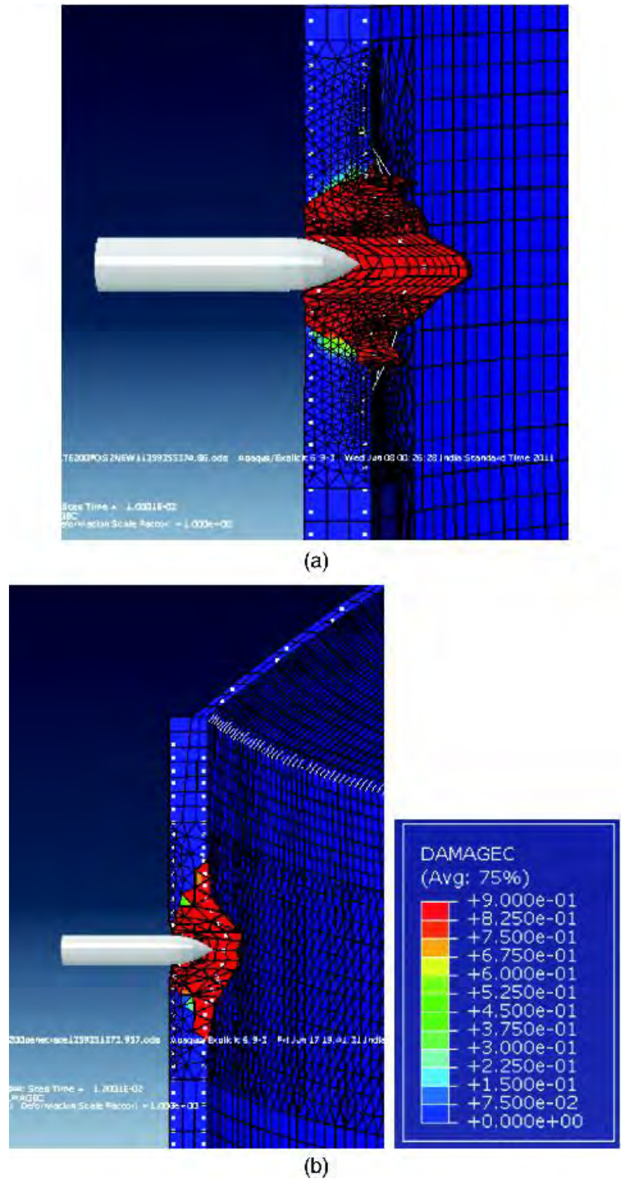

Fig. 11: Damage due to 200 m/s missile impact (a) at location1 (b) at location 2

5. Conclusions

Three dimensional numerical simulations are carried out using ABAQUS/Explicit finite element code to predict the response of typical containment structure under the direct hit of missile. The response of containment is studied for the missile impact at two different locations i.e., the junction of dome and cylinder and the midpoint of the cylinder. The following conclusions are drawn from the present study:

a) The difference in the response of containment due to incorporation of strain rate effect in the concrete model is studied. It is observed that there is nearly 40% decrement in the missile penetration depth in strain rate dependent model, as compared to that of strain rate independent model.

b) The penetration study is conducted on containment with 100 m/s and 200 m/s velocities. It is observed that, for the same missile velocity, missile penetrated to a higher depth at junction of dome and cylinder than that of at the centre of cylinder. An intense damage is observed at junction of dome and cylinder, where as a distributed damage is observed at centre of cylinder.

c) Present study illustrated that containment is capable to resist the impact of the missile under consideration.

6. Acknowledgements

The present work is part of the thesis carried out by the first author at Indian Institute of Technology, Roorkee. The authors would like to place on record and thank IIT Roorkee, for the support during the first author's tenure for carrying out this thesis for 'Master of Technology' in *Structural Engineering*.

References

1. Abaqus *6.9 Analysis User's Manual* Vol **1, 2, 3, 4, 5**
2. Abbas H, Paul D K, Godbole P N and Nayak G C Reaction-time response of aircraft crash *Comp Str* **5** (1995) 809-817
3. Borvik T, Hopperstad O S, Berstad T and Langseth M *Int J Impact Engg* **27** (2002) 37-64
4. Grote D L, Park S W and Zhou M Dynamic behaviour of concrete at high strain rates and pressures: experimental characterization *Int J Impact Engng* **25** (2001) 869-886
5. Hillerborg A, Moder M and Petersson P E Analysis of crack formation and crack growth in concrete by means of fracture mechanics and finite elements *Cement and Concrete Research* **6** (1976) 773-782
6. Jahnson G R and Cook W H Fracture Characteristics of Three Metals Subjected to Various Strain, Strain Rates, Temperatures and Pressures *J Engineering Fracture Mechanics* **21(1)** (1985) 31-48
7. Kukreja M Damage evaluation of 500 MWe Indian Pressurized Heavy Water Reactor nuclear containment for aircraft impact *Nucl Engg Des* **235** (2005) 1807-1817
8. Li Q M, Reid S R, Wen H M and Telford A R Local impact effects of hard missiles on concrete targets *The Int J Impact Engng* **32** (2005) 224-284
9. Lu Y and Xu K, Modelling of dynamic behaviour of concrete materials under blast loading *Int J Solids and Structures* **41** (2004) 131-143
10. Sinha B P, Gerstle K H and Tulin L G Stess-strain relations for concrete under cyclic loading *Jour American Concrete Institute* 195-211
11. Wolinski S, Hordijk D A, Reinhardt H W and Cornelissen H A W Influence of aggregate size on fracture mechanics parameters of concrete *The Inter J Cement Composites and Lightweight Concrete* **9(2)** (1987).